Implementation of a time-domain model for TALOS wave energy converter

W. Sheng, C. Michailides, E. Loukogeorgaki, and G. Aggidis

Abstract—**The TALOS wave energy converter is a novel point absorber-like wave energy converter (WEC), in which a unique power take-off (PTO) system is fully enclosed within the structure of the TALOS WEC (the hull), so to avoid direct contact with the harsh marine environment. This specific WEC is being investigated and developed at Lancaster University (UK), and the numerical modelling implementation of the TALOS wave energy converter is one of the main tasks of the Lancaster in-house time-domain analysis code.**

The PTO system of TALOS WEC consists of a heavy mass ball within the structure, which is linked with a number of linear springs and dampers to the hull of TALOS WEC for wave energy conversion. Such an arrangement of the PTOs could in principle convert the energy from all motion modes of the wave energy converter, but it would also make the PTO essentially non-linear, regardless the actual PTO damper's characteristics (linear or nonlinear). Therefore, a time domain analysis must be established for the TALOS WEC, which is the research work in this investigation.

Keywords— Multi-axis WEC, TALOS WEC, Time-domain analysis, two-body system.

I. INTRODUCTION

THE TALOS wave energy converter (WEC) is a novel wave energy converter, which was proposed and now is being developed at Lancaster University, UK [1, 2]. Figure 1 shows 3 shapes of different TALOS (a: octagonal, b: triangular and c: circular) and d) is the panels for the octagonal TALOS. In principle, the TALOS WEC is a point-absorber-like device, but with a very specific PTO system: the TALOS PTO system consists of a mass ball inside of the WEC, and the springs and PTO dampers are linked between the mass ball and the structure (see Figure 1b). Such an arrangement would make the TALOS a fully enclosed WEC, and no moving parts are exposed to the harsh marine environment, in a manner like other fully enclosed WECs, such as the SeaREV and other mass moving WECs [3, 4].

The PTO arrangement in TALOS WEC would also make the TALOS a factual multi-axis WEC, in a similar manner to other WECs using the multiple motion modes for wave energy conversions [5-7]. In principle, the TALOS device could convert wave energy through different motion modes of the structure, and this could provide an efficient conversion for wave energy.

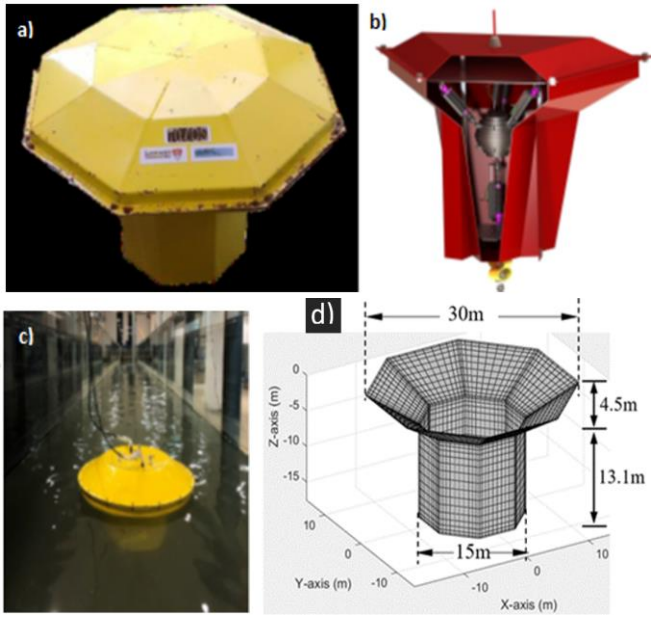

Figure 1 TALOS models: a) octagonal, b) triangular (and the PTO system), c) circular, and (d) the panels for the octagonal TALOS.

The challenges to model the TALOS WEC is the flexible connections between the structure and the ball, in which the structure motion is under the wave excitations, while

This work was partially supported by the UK Engineering and Physical Sciences Research Council (EPSRC grant number EP/V040561/1) for the project Novel High-Performance Wave Energy Converters with advanced control, reliability and survivability systems through machine-learning forecasting (NHP-WEC).

Wanan Sheng is with Renewable Energy Group, Lancaster University, UK (email: w.sheng@lancaster.ac.uk).

Constantine Michailides is with Department of Civil Engineering, International Hellenic University, Serres, University Campus, Greece. (email: cmichailides@ihu.gr)

Eva Loukogeorgaki is with Department of Civil Engineering, Aristotle University of Thessaloniki, Thessaloniki, Greece. (email: eloukog@civil.auth.gr)

George Aggidis is with Engineering Department at Lancaster University, Lancaster, UK. (e-mail: g.aggidis@lancaster.ac.uk).

Digital Object Identifier:
https://doi.org/10.36688/ewtec-2023-460

the ball motions is via the PTO forces/moments acting on the ball (acting on the structure too). To model the TALOS WEC, a numerical tool is being developed for this device, with the focus on how to best represent the mass-ball/springs/dampers PTO system. The links between the mass ball and the structure via the springs and PTO dampers would make the PTO essentially non-linear, regardless whether the actual PTO dampers are linear or nonlinear: the springs are generally linear, but PTO dampers can be either nonlinear or linear, depending on the actual PTO dampers. Therefore, a time domain analysis must be established for the TALOS WEC. Towards this goal, an in-house time-domain model is being developed and validated at Lancaster University.

To build a numerical model for TALOS WEC, the Lancaster in-house time-domain code is based on the hybrid frequency-time domain approach (see more details in [8] and [9]). That is, the basic frequency-domain hydrodynamic parameters are analysed using the popular panel codes, such as WAMIT, HAMS, NEMOH. Then the relevant frequency-dependent parameters are transformed for the Cummins' time-domain equation, such as the added mass at infinite frequency, and the memory effect (the convolution terms), as well as the wave excitation forces/moments.

The remaining sections are arranged as follows. In Section II, the description and the basic hydrodynamics of the TALOS WEC are given; in Section III, the time-domain approaches are formulated as the dynamics of a two-body system, via the PTO connections so for wave energy conversion; Section IV provides the calculations of the forces and moments acting on the mass ball and the hull, while in Section V, some results and the relevant analyses are given; and finally the conclusions are cited in Section VI.

II. HYDRODYNAMICS OF TALOS WEC

A. *TALOS energy conversion*

The TALOS WEC can be taken as a two-body system: one body is the hull of the structure, which interacts with the incoming waves and under the wave excitations the hull would move in 6-degrees of freedom (DOFs) as a rigid body, while the mass ball inside the hull would be linked to the hull via the springs and PTO dampers (see Figure 2 for an illustration). In wave energy conversion, the hull moves under the wave excitation, while the mass ball remains relatively stationary in an ideal situation, such that the relative motions between the hull and the mass ball could drive the PTO dampers to convert the wave energy into useful energy, such as the high-pressure flows using the hydraulic systems or the electricity using the direct drive.

B. *Frequency domain analysis of the hull in waves*

To study the hydrodynamic responses of the TALOS WEC, we can assume the mass ball in the TALOS is rigidly connected to the hull, such that the overall TALOS structure would have the correct draft and hydrodynamic features (see Figure 3).

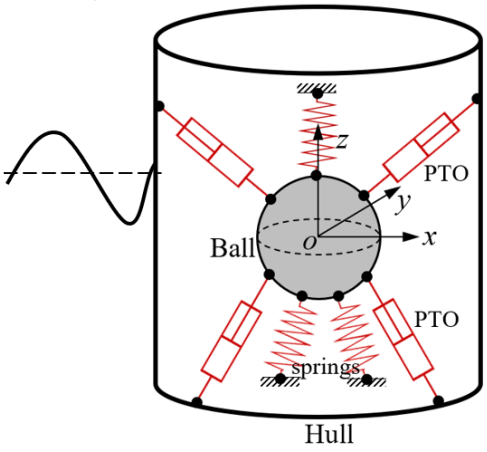

Figure 2 Multi-axis energy conversion system for TALOS

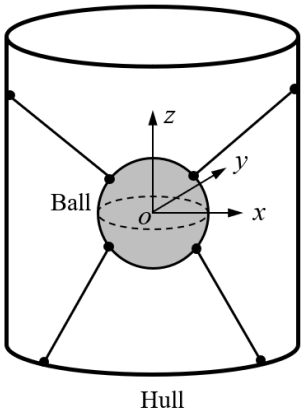

Figure 3 Hull and ball as a rigid body: the rigid connections between hull and ball

The hydrodynamics of the TALOS can be carried out using as a conventional panel method. Following WAMIT [10], the frequency-domain dynamic equation of 6-DOFs of a rigid structure is given in a form of mass-spring-damper system, as below:

$$\sum_{k=1}^{6}\{-\omega^2[M_{jk}+M_{jk}^E+A_{jk}(\omega)]+i\omega[B_{jk}(\omega)+B_{jk}^E]+(C_{jk}+C_{jk}^E)\}\xi_k(\omega)=F_j(\omega) \quad (1)$$

where ω is the circular frequency of the wave excitation, and the parameters with the variable ω mean their frequency dependency;

$M_{jk}, M_{jk}^E, A_{jk}(\omega)$ $(j,k = 1,2,\dots,6)$ are the structural, external and added mass matrices/coefficients, and the first two must be specified for the numerical modelling, while the last can be assessed using the panel method;

$B_{jk}(\omega), B_{jk}^E$ $(j,k = 1,2,\dots,6)$ are the radiation and external damping coefficients, with the first being assessed using the panel method, while the last must be specified in the numerical modelling;

C_{jk}, C_{jk}^{E} $(j,k = 1,2,\dots,6)$ are the hydrostatic and external restoring coefficients of the hull (both must be specified or calculated). The definition of the hydrostatic restoring coefficients C_{jk} can be found in WAMIT manual [10];

$F_j(\omega)(j = 1,2,\dots,6)$ is the frequency-dependent complex amplitude of the wave excitation, which can be calculated using the panel method;

$\xi_k(\omega)(k = 1,2,\dots,6,$ corresponding to the motions of surge, sway, heave, roll, pitch and yaw respectively) is the frequency-dependent complex amplitudes of motions of the floating structure, which are solved from the above dynamic equation. In applications, the response amplitude operator (RAO) is the more useful expression, defined as

$$\chi_k = \frac{\xi_k}{A} \tag{2}$$

where A is the wave amplitude (here the wave amplitude A is without a subscript or superscript). Obviously in the wave of a unit amplitude, the frequency-dependent ξ_k itself is the RAO.

III. TIME-DOMAIN DYNAMIC EQUATIONS

The interaction between the mass ball is considered as an independent rigid body. Hence the TALOS WEC is a two-body system: the hull of the TALOS device and the mass ball, with the PTO forces acting between them. In mathematical expressions, the motions of the hull and of the mass ball are linked through the forces and moments from the springs and the PTO dampers.

A. Dynamic equation for the hull

The mathematical equations for the hull motion in time domain are the hybrid frequency-time domain equations (see [8, 9]), where the fundamental hydrodynamic parameters are calculated based on the one-off frequency domain analysis, such as, the added mass at infinite frequency, the impulse functions and the excitation forces/moments (see details in [8]).

The motions in all 6-DOFs can be obtained by solving the time-domain equations, Eq. (3) below:

$$\begin{cases} m_s\ddot{x}_{h1}(t) + \sum_{j=1}^{6} A_{1j}\,\ddot{x}_{hj}(t) + \sum_{j=1}^{6}\int_0^t K_{1j}(t-\tau)\dot{x}_{hj}(\tau)d\tau + \sum_{j=1}^{6} C_{1j}\,x_{hj}(t) = F_1^{ex}(t) + F_{h1}^{pto}(t) + F_{h1}^{spr}(t) \\ m_s\ddot{x}_{h2}(t) + \sum_{j=1}^{6} A_{2j}\,\ddot{x}_{hj}(t) + \sum_{j=1}^{6}\int_0^t K_{2j}(t-\tau)\dot{x}_{hj}(\tau)d\tau + \sum_{j=1}^{6} C_{2j}\,x_{hj}(t) = F_2^{ex}(t) + F_{h2}^{pto}(t) + F_{h2}^{spr}(t) \\ m_s\ddot{x}_{h3}(t) + \sum_{j=1}^{6} A_{3j}\,\ddot{x}_{hj}(t) + \sum_{j=1}^{6}\int_0^t K_{3j}(t-\tau)\dot{x}_{hj}(\tau)d\tau + \sum_{j=1}^{6} C_{3j}\,x_{hj}(t) = F_3^{ex}(t) + F_{h3}^{pto}(t) + F_{h3}^{spr}(t) \\ I_{s44}\ddot{x}_{h4}(t) + \sum_{j=1}^{6} A_{4j}\,\ddot{x}_{hj}(t) + \sum_{j=1}^{6}\int_0^t K_{4j}(t-\tau)\dot{x}_{hj}(\tau)d\tau + \sum_{j=1}^{6} C_{4j}\,x_{hj}(t) = F_4^{exc}(t) + M_{h1}^{pto}(t) + M_{h1}^{spr}(t) \\ I_{s55}\ddot{x}_{h5}(t) + \sum_{j=1}^{6} A_{5j}\,\ddot{x}_{hj}(t) + \sum_{j=1}^{6}\int_0^t K_{5j}(t-\tau)\dot{x}_{hj}(\tau)d\tau + \sum_{j=1}^{6} C_{5j}\,x_{hj}(t) = F_5^{ex}(t) + M_{h2}^{pto}(t) + M_{h2}^{spr}(t) \\ I_{s66}\ddot{x}_{h6}(t) + \sum_{j=1}^{6} A_{6j}\,\ddot{x}_{hj}(t) + \sum_{j=1}^{6}\int_0^t K_{6j}(t-\tau)\dot{x}_{hj}(\tau)d\tau + \sum_{j=1}^{6} C_{6j}\,x_{hj}(t) = F_6^{ex}(t) + M_{h3}^{pto}(t) + M_{h3}^{spr}(t) \end{cases} \tag{3}$$

where

x_{hk} (k = 1, 2, …, 6) are the structure motions of 6 DOFs, which can be solved from the dynamic equation

A_{jk} (j, k = 1, 2, …, 6) the added mass/moment of inertia at infinite frequency (can be assessed based on the panel method)

K_{jk} (j, k = 1, 2, …, 6) the impulse functions (assessed based on the parameters from the panel method)

C_{jk} (j, k = 1, 2, …, 6) the hydrodynamic restoring coefficients (Panel method should include the assessment

F_j^{ex} (j = 1, 2, …, 6) the wave excitation forces and moments along and around x-, y- and z-axes, respectively

$F_{h(1,2,3)}^{pto}$ and $F_{h(1,2,3)}^{spr}$ are the forces acting on the hull from the PTOs and springs along x-, y- and z-axes, respectively (the calculations of the forces/moments from the PTO can be found in Section IV), and

$M_{h(1,2,3)}^{pto}$and $M_{h(1,2,3)}^{spr}$ are the moments acting on the hull from the PTOs and springs around x-, y- and z-axes, respectively.

B. Dynamic equation for the ball

The forces/moments acting on the mass ball are those PTO forces/moments, thus, the mathematical equations for the motions of the mass ball can be written as

$$\begin{cases} m_b\ddot{x}_{b1}(t) + B_{b1}\dot{x}_{b1}(t) = F_{b1}^{pto}(t) + F_{b1}^{spr}(t) \\ m_b\ddot{x}_{b2}(t) + B_{b2}\dot{x}_{b2}(t) = F_{b2}^{pto}(t) + F_{b2}^{spr}(t) \\ m_b\ddot{x}_{b3}(t) + B_{b3}\dot{x}_{b3}(t) = F_{b3}^{pto}(t) + F_{b3}^{spr}(t) \\ I_{b44}\ddot{x}_{b4}(t) + B_{b4}\dot{x}_{b4}(t) = M_{b1}^{pto}(t) + M_{b1}^{spr}(t) \\ I_{b55}\ddot{x}_{b5}(t) + B_{b5}\dot{x}_{b5}(t) = M_{b2}^{pto}(t) + M_{b2}^{spr}(t) \\ I_{b66}\ddot{x}_{b6}(t) + B_{b6}\dot{x}_{b6}(t) = M_{b3}^{pto}(t) + M_{b3}^{spr}(t) \end{cases} \tag{4}$$

with x_{bj} (j = 1, 2,…, 6) being the ball motions of 6 DOFs

m_b: the mass of the ball

I_{b44}, I_{b55}, I_{b66}: the moments of inertia of the ball (for a sphere, $I_{b44} = I_{b55} = I_{b66} = \frac{2}{5} m_b R^2$) with R being the radius of the sphere

B_{bj} (j = 1, 2,…, 6): the linear added damping coefficient for the mass ball motions

$F_{b(1,2,3)}^{pto}$ and $F_{b(1,2,3)}^{spr}$ are the forces acting on the ball from the PTOs and springs along x-, y- and z-axes, respectively, and

$M_{b(1,2,3)}^{pto}$ and $M_{b(1,2,3)}^{spr}$ are the moments acting on the ball from the PTOs and springs around x-, y- and z-axes, respectively.

IV. FORCES AND MOMENTS DUE TO PTOS

A. *Coordinates of connection points (for springs and dampers)*

To calculate the PTO forces and moments, the connection points, (x_b, y_b, z_b) on the mass ball and (x_h, y_h, z_h) on the hull, for the springs and PTO dampers must be calculated, see the illustration in Figure 4.

The roll (φ)-pitch (θ)-yaw (ψ) sequence of rotations is adopted following WAMIT, and the rotational matrix is calculated as

$$R = \begin{pmatrix} 1 & 0 & 0 \\ 0 & cos\varphi & -sin\varphi \\ 0 & sin\varphi & cos\varphi \end{pmatrix} \times \begin{pmatrix} cos\theta & 0 & sin\theta \\ 0 & 1 & 0 \\ -sin\theta & 0 & cos\theta \end{pmatrix} \times \begin{pmatrix} cos\psi & -sin\psi & 0 \\ sin\psi & cos\psi & 0 \\ 0 & 0 & 1 \end{pmatrix} \quad (5)$$

This rotation expression would be same for both rational motions of the hull and the ball. Here the rotational motions are defined as follows: for roll, $\varphi = x_{b4}$ or $\varphi = x_{h4}$ for the ball and the hull, respectively; and similarly, for pitch, $\theta = x_{b5}$ or $\theta = x_{h5}$ for the ball and the hull; and for yaw, $\psi = x_{b6}$ or $\psi = x_{h6}$ for the ball and the hull. In applications, a simplified rotational matrix is possible if the rotation angles are small, see details in WAMIT manual [10].

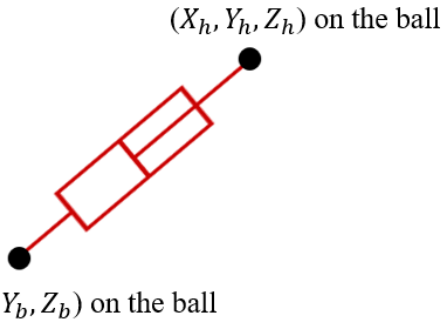

Figure 4 An illustration of the connection points (this is same for springs)

The position of the connection point (X_h, Y_h, Y_h) on the hull is calculated as:

$$\begin{pmatrix} X_h \\ Y_h \\ Z_h \end{pmatrix} = \begin{pmatrix} x_{h1} \\ x_{h2} \\ x_{h3} \end{pmatrix} + R \begin{pmatrix} x_{h0} \\ y_{h0} \\ z_{h0} \end{pmatrix} \quad (6)$$

Here x_{h1}, x_{h2}, x_{h3} are the translational motions of the hull (the solutions from Eq. 3), while (x_{h0}, y_{h0}, z_{h0}) is the original position of the connection point on hull when the hull is in the equilibrium position.

Similarly, the position of the connection point (X_b, Y_b, Z_b) on the ball would be calculated as

$$\begin{pmatrix} X_b \\ Y_b \\ Z_b \end{pmatrix} = \begin{pmatrix} x_{b1} \\ x_{b2} \\ x_{b3} \end{pmatrix} + R \begin{pmatrix} x_{b0} \\ y_{b0} \\ z_{b0} \end{pmatrix} \quad (7)$$

Here x_{b1}, x_{b2}, x_{b3} are the translational motions of the ball, while (x_{b0}, y_{b0}, z_{b0}) is the original position of the connection point on the ball when the ball in the equilibrium position.

The length between two connection points (on the hull and on the ball)

$$L = \sqrt{(X_h - X_b)^2 + (Y_h - Y_b)^2 + (Z_h - Z_b)^2} \quad (8)$$

And the original length (i.e., in calm water) is given as

$$L_0 = \sqrt{(x_{h0} - x_{b0})^2 + (y_{h0} - y_{b0})^2 + (z_{h0} - z_{b0})^2} \quad (9)$$

B. *Forces and moments due to PTO dampers*

Figure 5 shows the connecting points in the reference coordinate system and the corresponding forces acting on the connection points on the ball and on the hull.

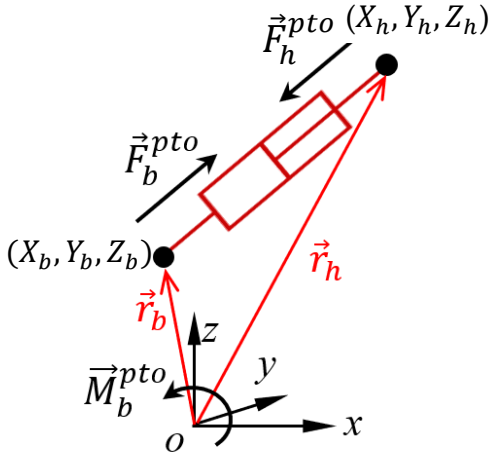

Figure 5 Force and moment calculation for the PTO

The vector for the two connection points (from the connection point on the ball to the connection point on the hull) would be given as

$$\Delta\vec{r} = \vec{r}_h - \vec{r}_b = (X_h - X_b)\vec{\imath} + (Y_h - Y_b)\vec{\jmath} + (Z_h - Z_b)\vec{k} \quad (10)$$

Obviously, this vector would be in the same direction with PTO force $\vec{F}_b^{pto}$ (shown in Figure 5).

For a linear PTO, its force F_b^{pto} along the PTO would be proportional to the PTO velocity, and it is calculated as

$$F_b^{pto}(t) = B_{pto} \frac{L(t) - L(t - \Delta t)}{\Delta t} \quad (11)$$

Here B_{pto} is the linear PTO coefficient; $L(t) = \sqrt{(X_h - X_b)^2 + (Y_h - Y_b)^2 + (Z_h - Z_b)^2}$ is the current length of the PTO, while $L(t - \Delta t)$ is the PTO length calculated in the same manner at the previous time step.

The PTO force components F_{b1}^{pto}, F_{b2}^{pto}, and F_{b3}^{pto} in x-, y- and z-directions acting on the ball in the coordinate o-xyz would be calculated as

$$\begin{cases} F_{b1}^{pto} = F^{pto}\left(\dfrac{X_h - X_b}{L}\right) \\ F_{b2}^{pto} = F^{pto}\left(\dfrac{Y_h - Y_b}{L}\right) \\ F_{b3}^{pto} = F^{pto}\left(\dfrac{Z_h - Z_b}{L}\right) \end{cases} \quad (12)$$

Obviously, the force components acting on the hull would be just in the opposite directions, as

$$\begin{cases} F_{h1}^{pto} = -F_{b1}^{pto} \\ F_{h2}^{pto} = -F_{b2}^{pto} \\ F_{h3}^{pto} = -F_{b3}^{pto} \end{cases} \tag{13}$$

The moment vector acting on the ball (with regard to the origin of the coordinate) due to the force $\vec{F}_b^{pto}$ would be calculated as

$$\begin{aligned} \vec{M}_b^{pto} = \vec{r}_b \times \vec{F}_b^{pto} &= \begin{bmatrix} \vec{\imath} & \vec{\jmath} & \vec{k} \\ X_b & Y_b & Z_b \\ F_{b1}^{pto} & F_{b2}^{pto} & F_{b3}^{pto} \end{bmatrix} \\ &= \left(Y_b F_{b3}^{pto} - Z_b F_{b2}^{pto}\right)\vec{\imath} \\ &+ \left(Z_b F_{b1}^{pto} - X_b F_{b3}^{pto}\right)\vec{\jmath} \\ &+ \left(X_b F_{b2}^{pto} - Y_b F_{b1}^{pto}\right)\vec{k} \end{aligned} \tag{14}$$

That is, the moment components are given as

$$\begin{cases} M_{b1}^{pto} = Y_b F_{b3}^{pto} - Z_b F_{b2}^{pto} \\ M_{b2}^{pto} = Z_b F_{b1}^{pto} - X_b F_{b3}^{pto} \\ M_{b3}^{pto} = X_b F_{b2}^{pto} - Y_b F_{b1}^{pto} \end{cases} \tag{15}$$

The moment acting on the hull would be calculated as

$$\begin{aligned} \vec{M}_h^{pto} = \vec{r}_h \times \left(-\vec{F}_b^{pto}\right) &= -(\vec{r}_b + \Delta\vec{r}) \times \vec{F}_b^{pto} \\ &= -\vec{r}_b \times \vec{F}_b^{pto} - \Delta\vec{r} \times \vec{F}_b^{pto} \\ &= -\vec{r}_b \times \vec{F}_b^{pto} = -\vec{M}_b^{pto} \end{aligned} \tag{16}$$

Note: $\Delta\vec{r}$ and $\vec{F}_b^{pto}$ are parallel, hence $\Delta\vec{r} \times \vec{F}_b^{pto} = 0$.

This means the moment acting on the hull is just in the opposite directions: the '$-$' sign is for the moment of PTOs in the dynamic equation of the hull.

C. *Forces and moments due to springs*

In a similar manner, the connecting points for the springs of the PTO (see Figure 6).

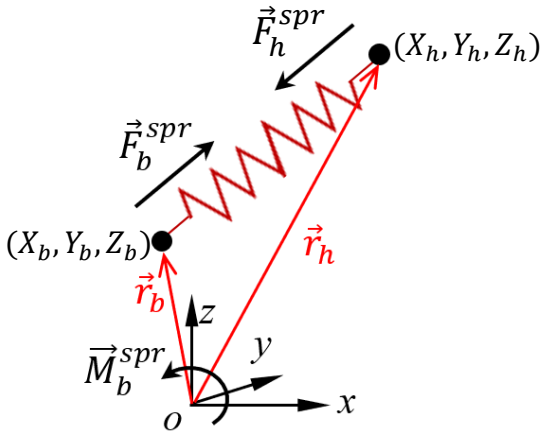

Figure 6 Force and moment calculation for the spring

For a spring, its force $\vec{F}_b^{spr}$ (magnitude) along the spring would be calculated as, with L_0 being the original length of the spring.

$$F_b^{spr}(t) = K[L(t) - L_0] \tag{17}$$

The spring force components F_{bx}^{spr}, F_{by}^{spr}, and F_{bz}^{spr} in x-, y- and z-directions acting on the ball in the $o-xyz$ coordinate system would be given as

$$\begin{cases} F_{bx}^{spr} = F_b^{spr}\left(\dfrac{X_h - X_b}{L}\right) \\ F_{by}^{spr} = F_b^{spr}\left(\dfrac{Y_h - Y_b}{L}\right) \\ F_{bz}^{spr} = F_b^{spr}\left(\dfrac{Z_h - Z_b}{L}\right) \end{cases} \tag{18}$$

Obviously, the force components acting on the hull would be just in the opposite directions, namely

$$\begin{cases} F_{hx}^{spr} = -F_{bx}^{spr} \\ F_{hy}^{spr} = -F_{by}^{spr} \\ F_{hz}^{spr} = -F_{bz}^{spr} \end{cases} \tag{19}$$

This is why in the dynamic equation for the hull, the PTO and spring forces have '-' signs.

The moment acting on the ball due to the force F would be calculated as

$$\begin{aligned} \vec{M}_b^{spr} = \vec{r}_b \times \vec{F}_b^{spr} &= \begin{bmatrix} \vec{\imath} & \vec{\jmath} & \vec{k} \\ X_b & Y_b & Z_b \\ F_{bx}^{spr} & F_{by}^{spr} & F_{bz}^{spr} \end{bmatrix} \\ &= \left(Y_b F_{bz}^{spr} - Z_b F_{by}^{spr}\right)\vec{\imath} \\ &+ \left(Z_b F_{bx}^{spr} - X_b F_{bz}^{spr}\right)\vec{\jmath} \\ &+ \left(X_b F_{by}^{spr} - Y_b F_{bx}^{spr}\right)\vec{k} \end{aligned} \tag{20}$$

Accordingly, the moment components are given as

$$\begin{cases} M_{bx}^{spr} = Y_b F_{bz}^{spr} - Z_b F_{by}^{spr} \\ M_{by}^{spr} = Z_b F_{bx}^{spr} - X_b F_{bz}^{spr} \\ M_{bz}^{spr} = X_b F_{by}^{spr} - Y_b F_{bx}^{spr} \end{cases} \tag{21}$$

In a similar manner, the moment acting on the hull would be just opposite as $\vec{M}_b^{spr}$, namely

$$\vec{M}_h^{spr} = -\vec{M}_b^{spr} \tag{22}$$

V. RESULTS AND ANALYSIS

In the following analysis, the PTO dampers and springs are assumed 6 (the spring and PTO damper have same connections on the ball and on the hull, as shown in Figure 1b): 3 springs/PTO dampers are uniformly located at the bottom of the ball and 3 are on the top of the ball, see the coordinates of the connection points in Table I. The reason for such an arrangement is that we need a large force from the springs to support the heavy ball, such that the all springs are not fully compressed. In this regard, the springs coefficients must be large enough, but the strong springs would make the PTO system too stiff, and thus, inefficient for wave energy conversion.

A target wave period of 10.0s (which roughly corresponds to the most occurred waves at West coast of Ireland, see the wave diagram in [11]), and wave height as 2.0m is taken as an example (Other parameters in the study are:

centre of gravity=-5.0m, and the linear mooring coefficients: C_{11}=C_{22}=5,000,000 N/m, C_{66}=10,000,000 Nm². For a practical purpose, the 6 springs have a restoring coefficient of 400,000 N/m. It can be seen that the wave energy conversion would increase with the increase of the PTO damper coefficient (see Table II). However, the increase of wave energy conversion would slow down when the PTO damping coefficient is larger than 150,000Ns/m.

Table I The connection coordinates on the ball and on the hull

on the ball			on the hull		
x	y	z	x	y	z
2.500	0.000	-4.330	5.000	0.000	-8.660
-1.250	2.165	-4.330	-2.500	4.330	-8.660
-1.250	-2.165	-4.330	-2.500	-4.330	-8.660
2.500	0.000	4.330	5.000	0.000	8.660
-1.250	2.165	4.330	-2.500	4.330	8.660
-1.250	-2.165	4.330	-2.500	-4.330	8.660

Table II The wave power conversions with TALOS WEC

K_0 (N/m)	B_{pto} (Ns/m)	P (kW)	T(s)/H(m)
400,000	25,000	146.6	10/2.0
400,000	50,000	186.8	*10/2.0*
400,000	75,000	228.3	10/2.0
400,000	100,000	298.4	10/2.0
400,000	150,000	380.4	10/2.0
400,000	250,000	429.3	10/2.0
400,000	500,000	543.9	10/2.0

The corresponding motions and the wave energy conversion can be seen in Figure 7 (K_0=400,000 N/m, B_{pto}=150,000 Ns/m). For a comparison, the hull motions ('black solid line, TD') and the ball motions ('green solid line, ball') are plotted, together with the hull motions of a free floating hull (with the mass ball fixed with the hull, 'dashed red line, FD'). For such a setup, the PTO springs are relatively strong, and the ball motions are large when compared to the hull motions (This is not an ideal situation, since the mass ball moves too much).

In terms of wave energy conversion, we can see the surge and pitch motions of the hull are reduced in magnitude, when compared to the free floating hull and the fixed mass (also see Figure 2), meaning that the energy has been taken out from these two motions modes, on the other hand the heave motion of the hull is increased slightly, which advocates that the heave motion may not contribute significantly to the energy absorption.

As a multi-axis WEC, the TALOS power conversion may not come to zero in a wave cycle (see Figure 7d), since there may be phase differences among the energy conversions from different DOFs.

Table III shows the trend of wave energy conversion using different spring coefficients, and it can be seen that the wave energy conversion would increase with the decrease of the spring coefficient. However, to support the mass ball in the appropriate position for wave energy conversion, the springs must be strong enough, but not too soft, since, in that case, the mass ball would sit on the fully compressed springs.

It should be noted that in all the above cases, the mooring system is quite stiff, such that the natural period of the surge motion is close to the natural period of pitch motion. In practice, such stiff mooring system may not be ideal. Using a softer mooring system (C_{11}=C_{22}=500,000 N/m, C_{66}=1,000,000 Nm²), the wave energy conversion by TALOS for would be reduced significantly, to 158kW (compared to 369kW for K_0=400,000 N/m, B_{pto}=150,000 Ns/m). The corresponding results are shown in Figure 8, where some low-frequency components in surge and pitch can be identified.

Table III The wave energy conversion using different spring coefficients

K_0 (N/m)	B_{pto} (Ns/m)	P (kW)	T(s)/H(m)
500,000	150,000	319.8	10/2.0
400,000	150,000	369.0	10/2.0
350,000	150,000	396.1	10/2.0
300,000	150,000	408.5	10/2.0
200,000	150,000	448.4	10/2.0

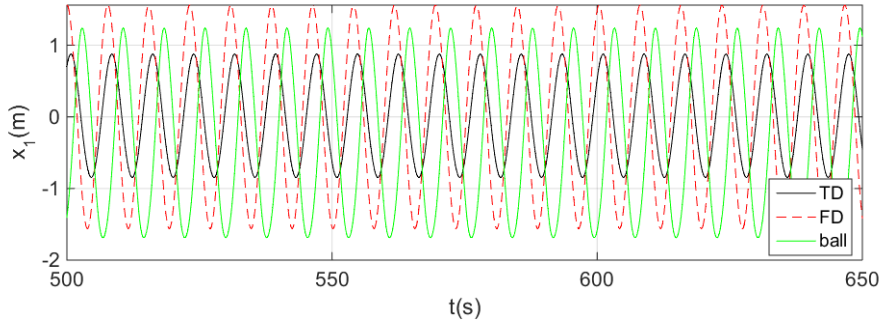

(a)

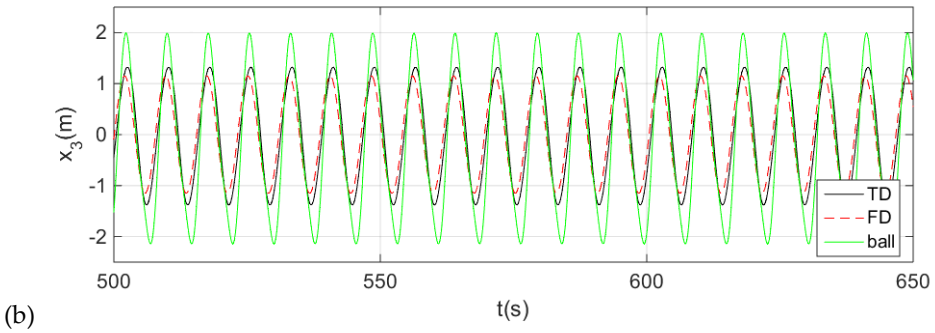

(b)

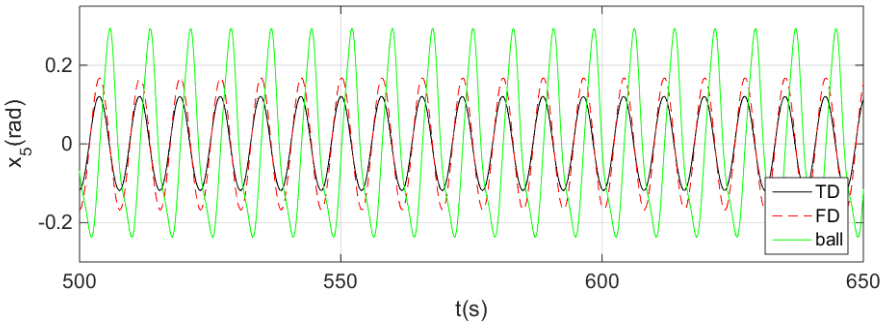

(c)

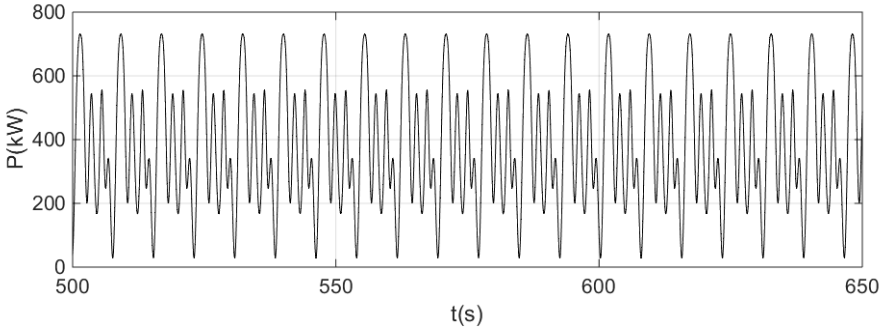

(d)

Figure 7 The motions of the hull and the mass ball and the power conversion. (a) surge, (b) heave, (c) pitch, (d) power conversion for a stiff mooring system C_{11}=C_{22}=5,000,000 N/m, C_{66}=10,000,000 Nm² and PTO with K_0=400,000 N/m and B_{pto}=150,000 Ns/m). . Legends: TD- time-domain solutions of the structure, FD- results directly based on frequency domain solutions (without PTOs)

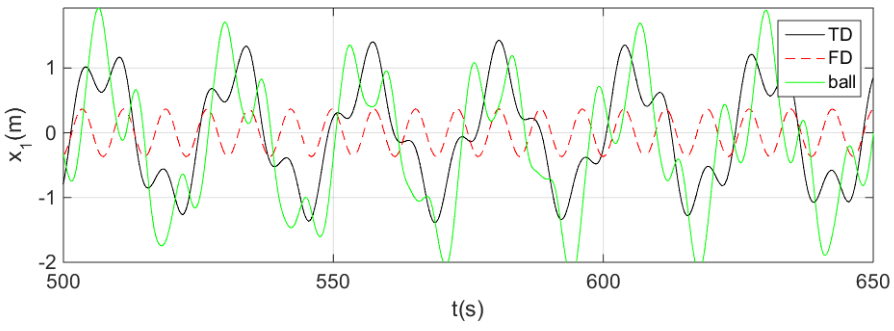

(a)

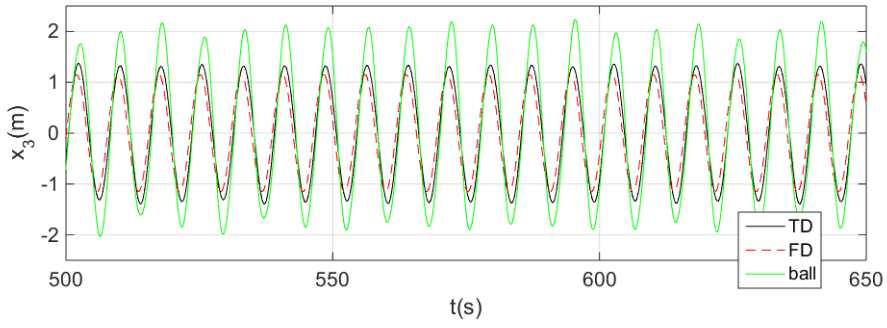

(b)

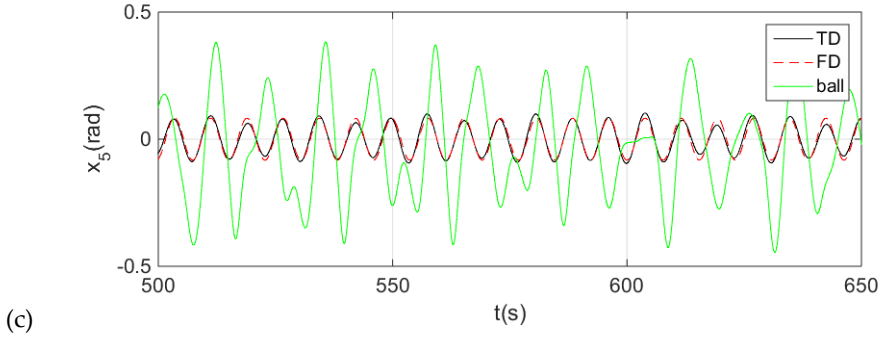

(c)

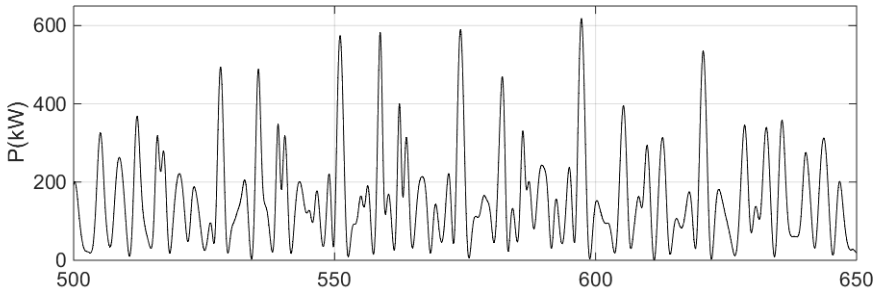

(d)

Figure 8 The motions of the hull and the mass ball and the power conversion. (a) surge, (b) heave, (c) pitch, (d) power conversion. On a softer mooring (C_{11}=C_{22}=500,000 N/m, C_{66}=1,000,000 Nm²) and PTO with K_0=400,000 N/m, B_{pto}=150,000 Ns/m. Legends: TD- time-domain solutions of the structure, FD- results directly based on frequency domain solutions (without PTOs).

VI. CONCLUSIONS

The main purposes of the work are to formulate the mathematical equation for the two-body system for TALOS WEC, and to initially study how the PTO springs and dampers could affect the wave energy conversion. Based on the results of the present analysis, the following conclusions can be derived:

- For a given PTO spring coefficient, the wave energy conversion increases with the increase of the PTO damping coefficient.
- For a given PTO damping coefficient, the wave energy conversion increases with the decrease of the PTO spring coefficient. However, the PTO springs must be chosen strong enough so to support the mass ball appropriately.
- A difficulty has been found in the multi-axis WEC that the surge motion is strongly coupled with the pitch motion and, thus, the wave energy conversion could be affected significantly by the mooring system.

Future work would include the validation of the present numerical model using other software packages, such as DNV SESAM and Chrono, as well as the experimental data; after that, the in-house time-domain analysis tool for TALOS would be used for optimising the TALOS WEC, including the PTO design and optimisation.

REFERENCES

1. Sheng, W., et al., *Hydrodynamic studies of floating structures: Comparison of wave-structure interaction modelling*. Ocean Engineering. **249**: p. 110878, 2022.
2. Aggidis, G.A. and C. Taylor, J., *Overview of wave energy converter devices and the development of a new multi-axis laboratory prototype.* IFAC PapersOnline. **50-1**: p. 15651-15656, 2017.
3. Cordonnier, J., et al., *SEAREV: Case study of the development of a wave energy converter.* Renewable Energy. **80**: p. 40-52, 2015.
4. Babarit, A., et al., *SeaRev: a fully integrated wave energy converter*. (cited on: 03/05/2015): http://192.107.92.31/test/owemes/29.pdf.
5. Tan, M., et al., *Power absorption modelling and analysis of a multi-axis wave energy converter.* IET Renewable Power Generation: p. 1-17, 2021.
6. Zhang, D., et al., *Wave tank experiments on the power capture of a multi-axis wave energy converter.* Journal of Marine Science and Technology,. **20**: p. 520-529, 2015.
7. Antoniadis, I.A., V. Georgoutsos, and A. Paradeisiotis, *Fully enclosed multi-axis inertial reaction mechanisms for wave energy.* Journal of Ocean Engineering and Science. **2**: p. 5-17, 2017.
8. Sheng, W., et al., *Time-Domain Implementation and Analyses of Multi-Motion Modes of Floating Structures.* Journal of Marine Science and Engineering. **10**: p. 662, 2022.
9. Taghipour, R., T. Perez, and T. Moan, *Hybrid frequency-time domain models for dynamic response analysis of marine structures.* Ocean Engineering. **35**(7): p. 685-705, 2008.
10. WAMIT, *User Manual (v73)*. (cited on: 01/11/2021): https://www.wamit.com/manualupdate/v73_manual.pdf.
11. Sheng, W. and G.A. Aggidis, *Fundamentals of Wave Energy Conversions*. Eliva Press, 2022.